Supplementary Information for Green Chemistry

Sustainability-inspired upcycling of waste polyethylene terephthalate (PET) plastic into porous carbon for CO_2 capture

Xiangzhou Yuan[a,b§], Nallapaneni Manoj Kumar[c§], Boris Brigljević[d§], Shuangjun Li[e], Shuai Deng[e], Manhee Byun[d], Boreum Lee[d], Carol Sze Ki Lin[c], Daniel C.W. Tsang[f], Ki Bong Lee[g], Shauhrat S. Chopra[c***], Hankwon Lim[d**], Yong Sik Ok[a*]

[a] *Korea Biochar Research Center, APRU Sustainable Waste Management Program & Division of Environmental Science and Ecological Engineering, Korea University, Seoul 02841, Republic of Korea*

[b] *R&D Centre, Sun Brand Industrial Inc., Jeollanam-do 57248, Republic of Korea*

[c] *School of Energy and Environment, City University of Hong Kong, Tat Chee Avenue, Kowloon, Hong Kong, China*

[d] *School of Energy and Chemical Engineering, Ulsan National Institute of Science and Technology, 50 UNIST-gil, Eonyang-eup, Ulju-gun, Ulsan 44919, Republic of Korea*

[e] *Key Laboratory of Efficient Utilization of Low and Medium Grade Energy (Tianjin University), Ministry of Education of China, Tianjin, China*

[f] *Department of Civil and Environmental Engineering, The Hong Kong Polytechnic University, Hung Hom, Kowloon, Hong Kong, China*

[g] *Department of Chemical and Biological Engineering, Korea University, Seoul 02841, Republic of Korea*

[§] These authors contributed equally as first authors.

Corresponding authors:

[*] Email: yongsikok@korea.ac.kr; [**] Email: hklim@unist.ac.kr; [***] Email: sschopra@cityu.edu.hk

Porous carbon sample synthesis

In this study, we synthesized three porous carbons from waste PET plastic bottles, using three different activation routes. First, based on a thermogravimetric analysis (TGA, TA Instruments Q50), we determined that waste PET plastic was carbonized at 600 °C for 1 h under an N_2 flow rate of 200 mL/min [S1]. The as-received sample was termed "PET6."

- CO_2 physical activation

  We loaded 5 g of PET6 into a horizontal tubular reactor (inner diameter 50 mm), then the reactor was heated to 900 °C (at a heating rate of 10 °C/min) and held at 900 °C for 2 h under a CO_2 flow rate of 200 mL/min. After the tubular reactor cooled from the operating temperature to room temperature, the as-received sample was named "PET6-CO_2-9."

- Potassium hydroxide (KOH) chemical activation [S1]

  A mixture of 5 g of PET6 and 10 g of KOH was added to 25 mL of deionized water at 60 °C for 1 h, and the mixture was then dried in a furnace at 110 °C overnight to remove the water. This dried mixture was further activated in a horizontal tubular reactor at 700 °C (heating rate of 10 °C/min) for 1 h under a N_2 flow rate of 200 mL/min, followed by treatment with a 0.5 N HCl solution to remove the remaining potassium component. After drying in a furnace at 110 °C overnight, the KOH-activated sample was collected and termed "PET6K7."

- KOH/urea co-activation [S1]

  Given that effective N-doping could enhance the uptake of and selectivity for CO_2 over other gases, we prepared N-doped porous carbon derived from waste PET plastic waste through a one-pot synthesis. We mixed 5 g of PET6 with KOH and urea (mass ratio of 1:2:1) in 25 mL of distilled water, and then dried the mixture in a furnace at 110 °C overnight to remove the water. The dried mixture was activated at 700 °C (heating rate of 10 °C/min) for 1 h under a N_2 flow rate of 200 mL/min. The same washing and drying treatments used for the previous activation method were applied, and the final sample was named "PET6KU7."

Clausius–Clapeyron equation

The isosteric heat of adsorption (Q_{st}), which can be used to measure the strength of the forces acting between the adsorbate molecules and the adsorbent surface, was calculated using the Clausius–Clapeyron equation (S1) [S2]. Information on the heat of adsorption is important for ensuring the correct equipment and process design.

$$Q_{st} = -R\left[\frac{\partial \ln p}{\partial\left(\frac{1}{T}\right)}\right]_{q_e} , \qquad (S1)$$

where R is the universal gas constant, T is the absolute temperature, and p is the pressure.

Energy consumption related indicators

The specific energy consumption E can be calculated based on the Carnot theorem:

$$E = w_{vac} + q_{heat}\left(\frac{T_{heat} - T_{cool}}{T_{heat}}\right) \qquad (S2)$$

where the specific work consumption w_{vac} represents the work consumed by the vacuum pump in the vacuuming step [S3]. The specific heat input q_{heat} in the heating step [S4] was calculated as follows:

$$w_{vac} = \frac{n_{vac}}{N_{CO_2,des}}\frac{22.4}{\eta_{vac}}\frac{k}{k-1}P_H\left[\left(\frac{P_H}{P_{vac}}\right)^{\frac{k-1}{k}} - 1\right] \qquad (S3)$$

$$Q_{heat} = (1-\varepsilon)V_{bed}\left[C_{p,ad}\left(T_H - T_L\right) + \rho_{ad}\left(\Delta n_{CO_2,des}\Delta H_1 + \Delta n_{N_2,des}\Delta H_2\right)\right] + V_w \qquad (S4)$$

$$q_{heat} = \frac{Q_{heat}}{N_{CO_2,des}M_{CO_2}} \qquad (S5)$$

where k and η_{vac} are the adiabatic coefficient of air and efficiency of the vacuum pump, respectively, and have values of 1.4, 0.7, respectively. M_{CO2} is the molar mass of the CO_2.

The exergy efficiency E_{ex} of the process was calculated as described below, with the minimum separation work w_{min} defined previously [S5,S6]. Therefore, the energy level used in the system can be evaluated.

$$E_{ex} = w_{min}/E \qquad (S6)$$

Ideal adsorption solution theory

Adsorption selectivity ($S_{i,j}$) for a binary mixture of CO_2 and N_2 was calculated by the ideal adsorption solution theory (IAST) using Eq. (S7) [S7]. In the selectivity calculation, it was assumed that only N_2 and CO_2 were involved, and the sum of the partial pressures of N_2 and CO_2 was equal to 1 atm.

$$S_{i,j} = \frac{q_i / p_i}{q_j / p_j} \qquad (S7)$$

where p_i and q_i represent the partial pressure and adsorption uptake of component i, respectively.

Detailed information for the 5-step TVSA

TVSA process is a typical temperature swing adsorption (TSA)-series process, in which the vacuuming is added into the TSA process as the additional step (as exhibited in **Figure S1**). Generally, in a 4-step TSA cycle, four steps (i.e., heating, cooling, pressurization, and adsorption) are considered. In the heating step, the CO_2 adsorbed releases from adsorbent when being heated up to the desorption temperature. In the cooling step, the temperature of adsorbent is cooled down, which is ready for CO_2 adsorption. In the pressurization step, the feed gas flows into one port of the adsorption column at a constant speed while the other port is closed, so the pressure of inside column increases. When reaching the adsorption pressure, the other port of the adsorption column is opened for the outflow of the N_2 waste, and the pressure of inside column stays at the adsorption pressure by a counterbalance valve until the adsorbent becomes saturated in the adsorption step. Moreover, as detailed described in **Table S2**, in

the 5-step TVSA process, the pressure decreases to the vacuuming pressure in the additional vacuuming step, which is determined by the selected vacuum pump.

Supporting information for discussion section

The ideal porous carbon for CO_2 capture has excellent CO_2 adsorption capacity, high selectivity, stable recyclability, fast adsorption/desorption kinetics, and facile regeneration [S8]. As presented in **Figure 1b**, **Figure S2**, **Figure 2**, and **Table S1**, varying the adsorption temperature, the highest CO_2 uptake values at 1 bar that could be attained was 6.25 mmol/g at 0 °C by PET6-CO_2-9, 4.58 mmol/g at 25 °C by PET6-KU7 and 2.82 mmol/g at 50 °C by PET6-KU7 [S1], demonstrating high applicability to the practical CO_2 capture process. Specifically, the N_2 adsorption isotherms of the three porous carbons (**Figure 2a-c**) indicate that the WPDPCs show good selectivity for CO_2 over N_2. Based on the pure gas isotherms, the ideal adsorbed solution theory (IAST, Eq. S7) was employed to evaluate the selectivity of CO_2 over N_2 of three samples in a flue gas mixture consisting of 10% CO_2 and 90% N_2 [S7]. The IAST CO_2 selectivity over N_2 of PET6-CO_2-9, PET6-K7, and PET6-KU7 was estimated to be 10.50, 13.52, and 18.29 at 25 °C, respectively. The PET6-KU7 demonstrated the highest CO_2 selectively over N_2 at 25 °C, which is similar to or higher than the selectivity of microporous carbons reported in previous studies [S7,S9,S10]. Moreover, the stable recyclability, fast adsorption/desorption kinetics, and facile regeneration were verified, as shown in **Figure 2d-f**. Based on these observations and lab-scale experimental data, we conclude that upcycling waste PET plastic bottles into porous carbons offers a promising pathway. The CO_2 capture process using WPDPCs is mainly dominated by physisorption, because 1) as shown in **Figure 2a-c**, the CO_2 uptake at a certain adsorption pressure decreased as the adsorption temperature was increased from 0 °C to 50 °C, indicating that physisorption dominates the CO_2 adsorption process [S1,S11-S13]; and 2)

all of the values of Q_{st} were less than 26 kJ/mol, corroborating that the CO_2 adsorption process was controlled by physisorption [S13,S14].

Table S1. *Physical properties and operation parameters of the system.*

Parameter	**Value**	**Unit**
Feed gas composition	0.2/0.8	vol% (CO_2/N_2)
Feed flow speed, v_{in}	1.05	m/s
Length of adsorption chamber, L	3000	mm
Outer diameter of the adsorption chamber	310	mm
Inner diameter of the adsorption chamber	300	mm
Number of finned tubes in each adsorption chamber	6	--
Outer diameter of the finned tube	25	mm
Inner diameter of the finned tube	20	mm
Fin height	13	mm
Fin spacing	8	mm
Overall heat transfer coefficient, h	100	J/(m^2 s K)
Bed heat capacity, $C_{p,ad}$	1	MJ/(m^3 K)
Chamber wall heat capacity, $C_{p,w}$	4	MJ/(m^3 K)

Table S2. *Physical phenomena that occur during the detailed steps of the temperature-vacuum swing adsorption (TVSA) process, as derived from a previous publication [S15].*

Steps	**Gas flow**	**Pressure**	**Temperature**
Pressurization	The feed gas (CO_2/N_2) flows into one port of the adsorption chamber at a constant speed (v_f).	As the other port is closed, the pressure inside the chamber rises from a low (PL) to a high value (P_H).	The adsorption heat is removed by the cooling medium to maintain the chamber at a constant temperature (T_L).
Adsorption	The feed gas (CO_2/N_2) flows in from one port of the adsorption chamber at a constant speed (v_f), while the other port is opened.	The pressure inside the chamber is maintained at a constant value (P_H).	The adsorption heat is removed by the cooling medium to maintain the chamber at a constant temperature (T_L)
Heating	The desorbed gas flows out from one port of the adsorption chamber, while the other port is closed.	The pressure inside the chamber is maintained the constant value (P_H).	The adsorption chamber is heated by the heating medium to attain the desorption temperature (T_H).
Vacuuming	The desorbed gas is drawn out by the vacuum pump from one port of the adsorption chamber, while the other port is closed.	Due to the continuous work of the vacuum pump, the pressure inside the chamber is decreased to attain the vacuuming pressure (P_{vac}).	The temperature of the adsorption chamber slightly decreases and is maintained at a constant temperature (T_{vac}).
Cooling	Both ports are closed; no gas flows into or out of the adsorption chamber.	As the temperature drops, the pressure inside the closed adsorption chamber further reduces to attain the desorption pressure (P_L).	The adsorption chamber is cooled down by the cooling medium to attain the adsorption temperature (T_L).

Table S3. *Governing equations group for steady-state modelling, as derived from a previous publication [S16].*

Step	Equations
Pressurization	$f_{\text{press}}^{\text{end}} = \frac{RT}{\varepsilon P_H}\left\{\frac{\varepsilon P_L}{RT}\left(f_{\text{cool}}^{\text{end}} - f_{in}\right) + \rho_{\text{ad}}\left(n_{1\text{cool}}^{\text{end}} - n_{1\text{press}}^{\text{end}}\right) + f_{in}\left[\frac{\varepsilon P_H}{RT} + \rho_{\text{ad}}\left(n_{1\text{press}}^{\text{end}} + n_{2\text{press}}^{\text{end}}\right) - \rho_{\text{ad}}\left(n_{1\text{cool}}^{\text{end}} + n_{2\text{cool}}^{\text{end}}\right)\right]\right\}$
	$t_{\text{press}} = \left[\frac{\varepsilon P_H}{RT} + \rho_{\text{ad}}\left(n_{1\text{press}}^{\text{end}} + n_{2\text{press}}^{\text{end}}\right) - \frac{\varepsilon P_L}{RT} - \rho_{\text{ad}}\left(n_{1\text{cool}}^{\text{end}} + n_{2\text{cool}}^{\text{end}}\right)\right]\frac{LRT_L}{P_H v_{in}}$
Adsorption	$t_{\text{ads}} = \frac{RT_L\left\{L\rho_{\text{ad}}\left[\left(n_{1\text{ads}}^{\text{end}} + n_{2\text{ads}}^{\text{end}}\right) + \left(n_{2\text{ads}}^{\text{end}} - n_{2\text{press}}^{\text{end}}\right) - \left(n_{1\text{press}}^{\text{end}} + n_{2\text{press}}^{\text{end}}\right)\right] + L\frac{\varepsilon P_H}{RT_L}\left(f_{\text{press}}^{\text{end}} - f_{\text{ads}}^{\text{end}}\right)\right\}}{v_{\text{in}} P_H f_{\text{in}}}$
Heating	$\left\{\frac{\varepsilon P}{RT} + \rho_{\text{ad}}\left[\left(1-f\right)\frac{\partial n_1}{\partial f} - f\frac{\partial n_2}{\partial f}\right]\right\}\frac{df}{dt} + \rho_{\text{ad}}\left[\left(1-f\right)\frac{\partial n_1}{\partial T} - f\frac{\partial n_2}{\partial T}\right]\frac{dT}{dt} = 0$
	$\left[C_{\text{p,ad}} + \rho_{\text{ad}}\left(\Delta H_1\frac{\partial n_1}{\partial T} + \Delta H_2\frac{\partial n_2}{\partial T}\right)\right]\frac{dT}{dt} + \rho_{\text{ad}}\left(\Delta H_1\frac{\partial n_1}{\partial f} + \Delta H_2\frac{\partial n_2}{\partial f}\right)\frac{df}{dt} = Sh\left(T_{heat} - T\right)$
Vacuuming	$\left[\left(\rho_{\text{ad}} f - \rho_{\text{ad}}\right)\frac{\partial n_1}{\partial T} + \rho_{\text{ad}} f\frac{\partial n_2}{\partial T}\right]\frac{dT}{dt} + \left[-\frac{\varepsilon f}{RT} + \left(\rho_{\text{ad}} f - \rho_{\text{ad}}\right)\frac{\partial n_1}{\partial f} + \rho_{\text{ad}} f\frac{\partial n_2}{\partial f}\right]\frac{df}{dt} + \left[\frac{\varepsilon f}{RT} + \left(\rho_{\text{ad}} f - \rho_{\text{ad}}\right)\frac{\partial n_1}{\partial P} + \rho_{\text{ad}} f\frac{\partial n_2}{\partial P}\right]\frac{dP}{dt} = 0$
	$\left[C_{\text{p,ad}} + \rho_{\text{ad}}\left(\Delta H_1\frac{\partial n_1}{\partial T} + \Delta H_2\frac{\partial n_2}{\partial T}\right)\right]\frac{dT}{dt} + \rho_{\text{ad}}\left(\Delta H_1\frac{\partial n_1}{\partial f} + \Delta H_2\frac{\partial n_2}{\partial f}\right)\frac{df}{dt} + \rho_{\text{ad}}\left(\Delta H_1\frac{\partial n_1}{\partial P} + \Delta H_2\frac{\partial n_2}{\partial P}\right)\frac{dP}{dt} = 0$
	$\left(\rho_{\text{ad}}\frac{\partial n_1}{\partial P} + \frac{\varepsilon f}{RT}\right)\frac{dP}{dt} + \left(\rho_{\text{ad}}\frac{\partial n_1}{\partial f} + \frac{\varepsilon P}{RT}\right)\frac{df}{dt} + \left(\rho_{\text{ad}}\frac{\partial n_1}{\partial T} - \frac{\varepsilon fP}{RT^2}\right)\frac{dT}{dt} = 0$
Cooling	$\left[\rho_{\text{ad}}\left(\frac{\partial n_1}{\partial P} + \frac{\partial n_2}{\partial P}\right) + \frac{\varepsilon}{RT}\right]\frac{dP}{dt} + \left[\rho_{\text{ad}}\left(\frac{\partial n_1}{\partial T} + \frac{\partial n_2}{\partial T}\right) - \frac{\varepsilon P}{RT^2}\right]\frac{dT}{dt} = 0$
	$\left[C_{\text{p,ad}} + \rho_{\text{ad}}\left(\Delta H_1\frac{\partial n_1}{\partial T} + \Delta H_2\frac{\partial n_2}{\partial T}\right)\right]\frac{dT}{dt} + \rho_{\text{ad}}\left(\Delta H_1\frac{\partial n_1}{\partial f} + \Delta H_2\frac{\partial n_2}{\partial f}\right)\frac{df}{dt} + \rho_{\text{ad}}\left(\Delta H_1\frac{\partial n_1}{\partial P} + \Delta H_2\frac{\partial n_2}{\partial P}\right)\frac{dP}{dt} = Sh\left(T_{cool} - T\right)$

Table S4. *Reference values from proximate and ultimate analyses of pure and waste polyethylene terephthalate (PET) samples and normalized calculated averages.*

Reference	S17	S18	S18	S19	S20	S21	S22	S23	S24	S25	*calculated*	*calculated*
PET sample information	Pure	Waste fibers	Waste textile	Waste containers and bottles	Pure	Pure	Pure	Pure	MSW*	Pure	*PET-pure (average)*	*PET-waste (average)*
Proximate analysis												
Moisture	0.0	0.0	1.4	0.5	0.0	0.1	0.1	0.0	0.5	0.0	*0.0*	*0.6*
Volatile	88.6	87.8	81.9	86.1	84.1	93.4	88.1	90.6	83.9	92.3	*89.8*	*84.9*
Fixed carbon	11.4	2.9	2.1	13.4	13.9	6.4	11.8	9.4	13.8	7.5	*10.1*	*8.1*
Ash	0.0	9.3	14.6	0.0	0.0	0.1	0.0	0.0	1.8	0.2	*0.0*	*6.4*
Ultimate analysis												
C	64.2	61.9	61.5	n.a	64.1	62.5	62.1	62.9	62.5	62.0	*63.1*	*67.8*
H	4.7	4.3	4.6	n.a	3.7	1.2	4.4	4.3	4.8	4.1	*3.7*	*5.0*
N	0.1	0.1	0.1	n.a	0.0	0.0	0.0	0.0	0.3	0.1	*0.0*	*0.2*
S	0.6	0.1	0.1	n.a	0.0	0.0	0.0	0.0	0.0	0.0	*0.1*	*0.1*
O	30.5	24.4	19.1	n.a	34.2	33.3	33.5	32.8	30.6	34.0	*33.1*	*27.0*

*MSW: Municipal solid waste.

Table S5. *Primary thermochemical conversion (slow pyrolysis) material balance for the process simulation (atomic balance error = 0.372%). The liquid/wax composition was estimated based on polyethylene terephthalate (PET) slow pyrolysis operating parameters (p, T, heating rate) from previously published studies and tuned to satisfy the atomic balance [S26-S28].*

Feedstock		Products (thermal decomposition at 5°C/min to 600°C + 1h at 600°C)					
PET, kg/h	1000	**Liquid/wax, kg/h**	547.6	CAS #	***B.P., °C, 1 atm	**Solid char, kg/h**	110
*PA %		Terephthalic acid, wt.%	5.86	100-21-0	392.4	UA, %	
Moisture	0.04	Benzoic acid, wt.%	24.36	65-85-0	249.2	C	93.70
Fixed carbon	10.11	4-Acetylbenzoic acid, wt.%	11.41	586-89-0	340.0	H	0.10
Volatile matter	89.85	4-Methylbenzoic acid, wt.%	2.15	99-94-5	275.3	N	0.10
Ash	0.05	4-Ethylbenzoic acid, wt.%	0.86	619-64-7	270.3	S	0.80
**UA, %		4-Phenylbenzoic acid, wt.%	45.14	92-92-2	372.6	O	4.90
C	63.03	4-Hydroxybenzoic acid, wt.%	0.07	99-96-7	336.2	Ash	0.40
H	3.72	2-Naphthoic acid, wt.%	5.68	93-09-4	332.9	**Gas, kg/h**	342.4
N	0.02	Dibutyl phthalate, wt.%	0.75	84-74-2	337.0	CO, wt.%	45.13
S	0.09	Biphenyl, wt.%	0.55	92-52-4	255.0	CO_2, wt.%	49.57
O	33.09	Phenantrene, wt.%	0.62	85-01-8	337.4	H_2, wt.%	2.95
Ash	0.05	p-Terphenyl, wt.%	2.54	92-94-4	400.0	CH_4, wt. %	2.36

*PA: Proximate analysis; **UA: Ultimate analysis; ***BP: Boiling point.

The gate-to-gate life-cycle assessments (LCA) of the three adsorbent materials were modelled to compute the global warming potential (GWP) and other impact categories (see below) by taking into account the quantity of materials used in each activation process (CO_2, KOH, urea, HCl) **(Table S9).** The emissions due to energy requirement is not accounted, as the industrial facility is planned to have captive power plant (i.e., waste heat to electricity unit).

Table S6. *Summary of carbon activation process life cycle inventory (LCI) data of 1 kg of captured CO_2 by polyethylene terephthalate (PET)-derived porous carbon.*

Description	**PET6-CO_2-9**	**PET6-K7**	**PET6-KU7**
Activation method	CO_2 Physical Activation	KOH Chemical Activation	KOH/Urea Chemical Activation
Input materials	CO_2: 502.65 kg	KOH: 154.17 kg HCl: 292.96 kg/h	KOH: 118.53 kg HCl: 225.24 kg Urea: 64.76 kg
Electricity	302.2780 kW	222.6496 kW	171.2984 kW

Table S7. *List of impact categories.*

Impact category	**Unit**
Global warming	kg CO_2 eq
Stratospheric ozone depletion	kg CFC11 eq
Ionising radiation	kBq Co-60 eq
Ozone formation, human health	kg NO_x eq
Fine particulate matter formation	kg $PM_{2.5}$ eq
Ozone formation, terrestrial ecosystems	kg NO_x eq
Terrestrial acidification	kg SO_2 eq
Freshwater eutrophication	kg P eq
Marine eutrophication	kg N eq
Terrestrial ecotoxicity	kg 1,4-DCB
Freshwater ecotoxicity	kg 1,4-DCB
Marine ecotoxicity	kg 1,4-DCB
Human carcinogenic toxicity	kg 1,4-DCB
Human non-carcinogenic toxicity	kg 1,4-DCB
Land use	m2a crop eq
Mineral resource scarcity	kg Cu eq
Fossil resource scarcity	kg oil eq
Water consumption	m^3

To carry out the techno-economic analysis (TEA), we required details on the equipment and other associated costs for a 1 t/h waste PET treatment plant. The total capital cost details are provided in **Table S8**. Data collection was done based on each process. The scaled model was subdivided into different processes: pre-treatment, pyrolysis, carbon activation process, power generation, flue gas treatment, miscellaneous expenses and infrastructure cost. The sum of all of these process costs was considered to represent the total capital investment (TCI).

Table S8. *List of equipment and associated costs (CAPEX) for a 1 t/h waste polyethylene terephthalate (PET)-derived porous carbon production plant.*

Equipment cost	**Capacity**			**Cost**			**Reference or Source**
	PET6-CO_2-9	***PET6-K7***	***PET6-KU7***	***PET6-CO_2-9***	***PET6-K7***	***PET6-KU7***	
Waste PET Pre-treatment Cost							
Weighbridges	50 t			€ 21,500.00			S29
Feedstock store	1500 t			€ 5,680.50			S30
Belt conveyer system	10 m			€ 1,700.00			*
Shredder	1 t			€ 7,682.40			S31
Trommel screen with conveyers	1 t			€ 18,000.00			*
Loading shovels	0.5 t			€ 11,250.00			*
Excavator	0.5 t			€ 11,250.00			*
Sub-total: 1 (ST1)				*€ 77062.90*			-
Pyrolysis Unit							
Auger screw-flue gas heated pyrolizer with vapour collection	1 t/h			€ 799,044.80			S32
Auger conveyor belt	5 m			€ 840.00			*
Horizontal belt conveyors motors	3 motors	5 motors		€ 360.00	€ 600.00		*
Sub-total: 2 (ST2)				*€ 800,244.80*	*€ 800,484.80*		-
Carbon Activation Process							
Activation reactor	0.11 t			€ 3,200.00			*
KOH solution storage tank	15 t			€ 780.00			*
Urea solution storage tank	6 t			€ 320.00			*
HCL solution storage tank	20 t			€ 1,040.00			*
Mixing tank	-	1 t	2 t	-	€ 3,500.00	€ 7,000.00	*
Dryer		2		-	€ 8,000.00		*
Washer	-	1		-	€ 5,000.00		*

Silo/Bin (Porous carbon storage)	2.5 t	€ 1,600.00			*
Sub-total: 3 (ST3)		*€ 6,940.00*	*€ 23,440.00*	*€ 26,940.00*	-
Power Generation					
High pressure turbine	306.6 kW	€ 246,636.00			S29
Medium pressure turbine	347.8 kW	€ 280,326.80			S29
Low pressure turbine	614.6 kW	€ 495,367.50			S29
Organic Rankine cycle turbine	95.4 kW + 5 t (Working fluid)	€ 571,323.62			S33,S34, *a
Water chiller unit	5 t/h	€ 5,725.00			*
Cold water storage tank	150 t	€ 30,750.00			*
Sub-total: 4 (ST4)	*1341.97 kW*	*€ 1,630,128.92*			-
Flue gas treatment € 20,388.62					
Pressure swing adsorption unit and associated components	1 unit (20 kg/h to 300 kg/h)	€ 203,950.00			*
Sub-total: 5 (ST5)		*€ 203,950.00*			-
Miscellaneous expenses					
Additional machinery	-	€ 82,950.00			S35
Sub-total: 6 (ST6)		*€ 82,950.00*			-
Infrastructure costs					
Land cost	12,000 m^2 at €93.60/m^2	€ 1,123,200.00			Estimated
Office and laboratory equipment	-	€ 400,000.00			S35
Buildings	-	€ 200,000.00			Estimated
Sub-total: 7 (ST7)		*€ 1,723,200.00*			-
Total Capital Investment (TCI) = ST1+ST2+ST3+ST4+ST5+ST6+ST7	-	**€ 4,524,476.62**	**€ 4,541,186.62**	**€ 4,544,716.62**	-

Note: * denotes data from https://www.alibaba.com/. All of the values were converted from RMB to Euros at a conversion rate RMB 1 = € 0.13; [a] represents the cost value for the working fluid.

The operational cost details were estimated after accounting for the material input required for the three-activation processes. The carbon required to ensure that the production unit remained burden free, and the other infrastructure overhead recurring charges are presented in **Table S9**. We obtained operational data based on the process requirement. Energy consumption was the most commonly required input required, which was supplied internally through the CHP plant. The net-energy efficiency of the CHP system ensured that the cost related to energy consumptions was negligible. The cost data related to consumables, especially those used for the activation process, were obtained from the suppliers and through Alibaba, the Internet company with which the long-term contracts were drawn.

The water required for the power generation process was obtained on a monthly basis from the Tianjin Industrial Use Water Suppliers at a price of RMB7.9/t (the price is regulated by the Price Monitoring Center, NDRC) [S36]. For the operational costs, the cost involved in capturing the released CO_2 emissions was also considered by taking into account the cost values for the purchased porous carbons.

Table S9. *List of operational costs for a 1 t/h waste polyethylene terephthalate (PET) derived porous carbon production plant (annual operating hours = 8000 h).*

Equipment cost	**Capacity**			**Cost**			**Reference or Source**
	PET6-CO_2-9	***PET6-K7***	***PET6-KU7***	***PET6-CO_2-9***	***PET6-K7***	***PET6-KU7***	
Carbon Activation Process							
CO_2 gas	1.05 t/h	-	-	0.00 [a]	-	-	-
KOH	-	0.421 t/h		-	€ 232.00		*
Urea	-	-	0.23 t/h	-	-	€ 57.00	*
HCL	-	0.8 t/h		-	€ 174.67		*
Sub-total: 8 (ST8) [c]	*Estimated per year*			-	*€ 3,253,360.00*	*€ 3,709,360.00*	-
Power Generation							
Water	*3.9 t/h*			€ 3.89			[S36]
Sub-total: 9 (ST9) [c]	*Estimated per year*			*€ 31,120.00*			-
Flue Gas Treatment							
Energy	Energy from the combined heat and power plant within the system boundary						
Capture cost for plant emission [b]	76 t	66 t	46 t	€ 95,852.16	€ 83,005.56	€ 57,852.36	Estimated
Sub-total: 10 (ST10)				*€ 95,852.16*	*€ 83,005.56*	*€ 57,852.36*	-
Human Resource							
Workforce includes plant operators, administrative team etc.	Salaries and other expenses for 15 people per year			€ 126,096.17			Estimated
Sub-total: 11 (ST11) [c]	*Estimated per year*			*€ 126,096.17*			-

Miscellaneous Expenses [c]					
Maintenance	6% of TCI	€ 271,468.59	€ 272,471.19	€ 272,682.99	[37]
Insurance	2.5% of TCI	€ 113111.92	€ 113,529.67	€ 113,617.92	[38]
Contingencies	5% of TCI	€ 226223.83	€ 227,059.33	€ 227,235.83	[39]
ICT infrastructure cost	Per year	€ 5,000.00			Estimated
Sub-total: 12 (ST12)	*Estimated per year*	€ 615,804.34	€ 618, 060.19	€ 618,536.74	
First Year Operation Cost (FYOC)= ST8+ST9+ST10+ST11+S12	*Estimated per year (first year)*	*€ 868,872.67*	€ 4,111,641.92	*€ 4,542,965.27*	-
Yearly Operation Cost (YOC)= ST8+S9+ST11+S12	*Estimated per year (Second year onwards)*	*€ 773,020.51*	*€ 4,028,636.36*	*€ 4,485,112.91*	-

[a] the required CO_2 for physical activation was obtained from the pressure swing adsorption (PSA) unit; [b] one time cost in the first year only; [c] yearly expenses; * denotes data obtained from https://www.alibaba.com/; All the values were converted from RMB to Euro at a conversion rate of RMB 1 = € 0.13.

From the proposed porous carbon production unit, revenues can be generated by selling the produced porous carbon and excess electricity from the combined heat and power (CHP) plant. The revenue streams are based on the period of plant operation (8000 h). Therefore, the pricing of porous carbon, especially in the Chinese market, should take into account. It has been observed that cost of the porous carbon varies as per the current market, the price range of 1 ton of porous carbon is between € 286.30 and € 2,862.99 (https://www.alibaba.com/). Besides from the sale of porous carbon, the sale of electricity sales at the feed-in-tariff rates was also found to be favourable owing to China's unified pricing scheme. In China, the national unified feed-in tariff of waste-to-energy projects, such as waste PET-derived combined heat and power plants, is set at $0.106/kWh (€0.086/kWh) [S40]. The conversion to Euros was done as per the market value on 7th January 2021. There has been rising interest in carbon trading in China; therefore, we have considered the revenues generated by offsetting electricity (1.1082 tCO_2/kWh is the current emission factor for the Northeast China Power Grid). The carbon price in the Tianjin region is currently RMB 10-15/ton of CO_2eq. The pricing of the revenue parameters is given in **Table S13.**

Table S10*.Revenue parameters.*

Parameters	**Cost/value**	**Remark**	**References**
Porous carbon selling price (1 ton)	€ 286.30	Minimum selling price [d]	*
	€ 2,862.99	Maximum selling price [d]	*
Electricity selling price (1 kWh)	€0.086 /kWh	National unified feed-in tariff of waste-to-energy projects [d]	[S40]

* denotes the data obtained from https://www.alibaba.com/. All of the values were converted from RMB to Euros at conversion rate of RMB 1 equals €0.13; [d] represents the market price (MP).

Table S11. *Revenue generation by sales of the porous carbon (in Euro).*

Year	Porous carbon (ton)			Revenue (when sold at the minimum price)			Revenue (when sold at an average price)			Revenue (when sold at the maximum price)		
	PET6-CO_2-9	PET6-K7	PET6-KU7	PET6-CO_2-9	PET6-K7	PET6-KU7	PET6-CO_2-9	PET6-K7	PET6-KU7	PET6-CO_2-9	PET6-K7	PET6-KU7
1	704	800	720	201,555.20	229,040.00	206,136.00	1,107,494.08	1,259,716.00	1,133,744.40	2,015,544.96	2,290,392.00	2,061,352.80
2	704	800	720	201,555.20	229,040.00	206,136.00	1,107,494.08	1,259,716.00	1,133,744.40	2,015,544.96	2,290,392.00	2,061,352.80
3	704	800	720	201,555.20	229,040.00	206,136.00	1,107,494.08	1,259,716.00	1,133,744.40	2,015,544.96	2,290,392.00	2,061,352.80
4	704	800	720	201,555.20	229,040.00	206,136.00	1,107,494.08	1,259,716.00	1,133,744.40	2,015,544.96	2,290,392.00	2,061,352.80
5	704	800	720	201,555.20	229,040.00	206,136.00	1,107,494.08	1,259,716.00	1,133,744.40	2,015,544.96	2,290,392.00	2,061,352.80
6	704	800	720	201,555.20	229,040.00	206,136.00	1,107,494.08	1,259,716.00	1,133,744.40	2,015,544.96	2,290,392.00	2,061,352.80
7	704	800	720	201,555.20	229,040.00	206,136.00	1,107,494.08	1,259,716.00	1,133,744.40	2,015,544.96	2,290,392.00	2,061,352.80
8	704	800	720	201,555.20	229,040.00	206,136.00	1,107,494.08	1,259,716.00	1,133,744.40	2,015,544.96	2,290,392.00	2,061,352.80
9	704	800	720	201,555.20	229,040.00	206,136.00	1,107,494.08	1,259,716.00	1,133,744.40	2,015,544.96	2,290,392.00	2,061,352.80
10	704	800	720	201,555.20	229,040.00	206,136.00	1,107,494.08	1,259,716.00	1,133,744.40	2,015,544.96	2,290,392.00	2,061,352.80
11	704	800	720	201,555.20	229,040.00	206,136.00	1,107,494.08	1,259,716.00	1,133,744.40	2,015,544.96	2,290,392.00	2,061,352.80
11	704	800	720	201,555.20	229,040.00	206,136.00	1,107,494.08	1,259,716.00	1,133,744.40	2,015,544.96	2,290,392.00	2,061,352.80
13	704	800	720	201,555.20	229,040.00	206,136.00	1,107,494.08	1,259,716.00	1,133,744.40	2,015,544.96	2,290,392.00	2,061,352.80
14	704	800	720	201,555.20	229,040.00	206,136.00	1,107,494.08	1,259,716.00	1,133,744.40	2,015,544.96	2,290,392.00	2,061,352.80
15	704	800	720	201,555.20	229,040.00	206,136.00	1,107,494.08	1,259,716.00	1,133,744.40	2,015,544.96	2,290,392.00	2,061,352.80
Lifetime	10,560 t	12,000 t	10,800 t	€ 3,023,328.00	€ 3,435,600.00	€ 3,092,040.00	€ 16,612,411.20	€ 18,895,740.00	€ 17,006,166.00	€ 30,233,174.40	€ 34,355,880.00	€ 30,920,292.00

The revenue earned by selling electricity was estimated by considering heat loss scenarios, as shown in **Table S12**.

Table S12. *Heat loss scenarios resulting in power output losses.*

Parameters	**PET6-CO_2-9**					**PET6-K7**					**PET6-KU7**				
Total Q loss; %	1.00	10.00	20.00	50.00	75.00	1.00	10.00	20.00	50.00	75.00	1.00	10.00	20.00	50.00	75.00
Tfg (Rankine in); C	1202.00	1185.00	1167.00	1113.00	1067.00	1259.00	1243.00	1225.00	1170.00	1125.00	1245.00	1228.00	1208.00	1150.00	1100.00
Rankine H_2O; kg/h	4010.00	3915.00	3810.00	3490.00	3220.00	3925.00	3845.00	3750.00	3460.00	3220.00	3850.00	3760.00	3655.00	3345.00	3085.00
Net; kW	706.56	678.25	646.97	551.55	470.99	706.56	682.80	654.53	568.00	496.50	703.35	676.60	645.25	552.84	475.31
Act Q; MJ/h	-581.42	-581.42	-581.42	-581.42	-581.42	-252.89	-252.89	-252.89	-252.89	-252.89	-486.0596	-486.06	-486.06	-486.06	-486.06
Pyro Q; MJ/h	-2859.14	-2859.14	-2859.14	-2859.14	-2859.14	-2859.14	-2859.14	-2859.14	-2859.14	-2859.14	-2859.136	-2859.14	-2859.14	-2859.14	-2859.14
Cooling water; kg/h	4043.00	3971.00	3878.00	3623.00	3403.00	3983.00	3910.00	3831.00	3600.00	3411.00	3799.00	3712.00	3639.00	3385.00	3175.00
Act Q Loss; MJ/h	-5.81	-58.14	-116.28	-290.71	-436.07	-2.53	-25.28	-50.578	-126.45	-189.68	-4.86	-48.61	-97.22	-243.03	-364.55
Pyro Q Loss; MJ/h	-28.60	-285.91	-571.83	-1429.57	-2144.35	-28.60	-285.91	-571.83	-1429.57	-2144.35	-28.59	-285.91	-571.83	-1429.57	-2144.35

Table S13. *Revenue generation by sales of electricity (in Euro).*

Sample	Lifetime varying different heat loss percentage					
	0%	**1%**	**10%**	**20%**	**50%**	**75%**
PET6-CO_2-9	85,200,000	84,787,200	81,390,000	77,636,400	66,186,000	56,518,800
PET6-K7	87,988,800	84,787,200	81,936,000	78,543,600	68,160,000	59,580,000
PET6-KU7	87,988,800	84,402,000	81,192,000	77,430,000	66,340,320	57,036,960

Table S14.

Textural property, ultimate analysis, and CO_2 uptake of waste polyethylene terephthalate (PET) plastic-derived porous carbons.

Samples	S_{BET}[a]	V_{total}[b]	V_{micro}[c]	V_{micro}/V_{total}	Atomic (%)[d]			CO_2 uptake (mmol/g)[e]		
	m^2/g	cm^3/g			C	O	N	0 °C	25 °C	50 °C
PET6-CO_2-9	1482	0.607	0.592	0.975	92.99	7.11	-	6.25	3.63	2.29
PET6-K7 *	1263	0.519	0.501	0.965	93.27	6.73	-	5.30	3.87	2.29
PET6-KU7 *	1165	0.469	0.460	0.981	77.97	18.80	3.23	6.23	4.58	2.82

[a] calculated using the Brunauer-Emmett-Teller model.

[b] total pore volume at p/p0 = 0.99 from the Horvath-Kawazoe equation.

[c] micropore volume from the Dubinin-Radushkevich Equation.

[d] calculated from the corresponding peak areas of the X-ray photoelectron spectroscopy (XPS) spectra.

[e] obtained at 1 bar using a volumetric sorption analyzer.

* experimental data obtained from a previous publication [S1].

Table S15.

Process operation conditions and performance evaluation.

Operation parameters	**Value**			**Unit**
Heating medium temperature, T_{heat}	120			^{o}C
Cooling medium temperature, T_{cool}	25			^{o}C
Heat transfer temperature difference	5			^{o}C
Adsorption pressure, P_{H}	1.0			bar
Vacuuming pressure, P_{vac}	0.1			bar
Performance indicators	**PET6-CO_2-9**	**PET6-K7**	**PET6-KU7**	
Productivity	32.88	27.03	44.23	kg/t h
Purity	70.52	71.57	77.73	%
Recovery	89.88	84.93	90.02	%
Specific energy consumption, E	1.04	1.44	0.97	GJ/t
Exergy efficiency, E_{ex}	7.21	5.06	8.94	%

TVSA	Pressurization	Adsorption	Heating	Vacuuming	Cooling
Detailed steps	 Dry feed	N_2 waste  Dry feed	Heating medium 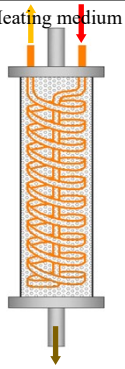 CO_2 product	 CO_2 product	Cooling medium 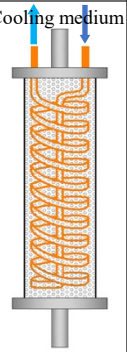

Figure S1. *Schematic diagram of the 5-step temperature-vacuum swing adsorption (TVSA) process.*

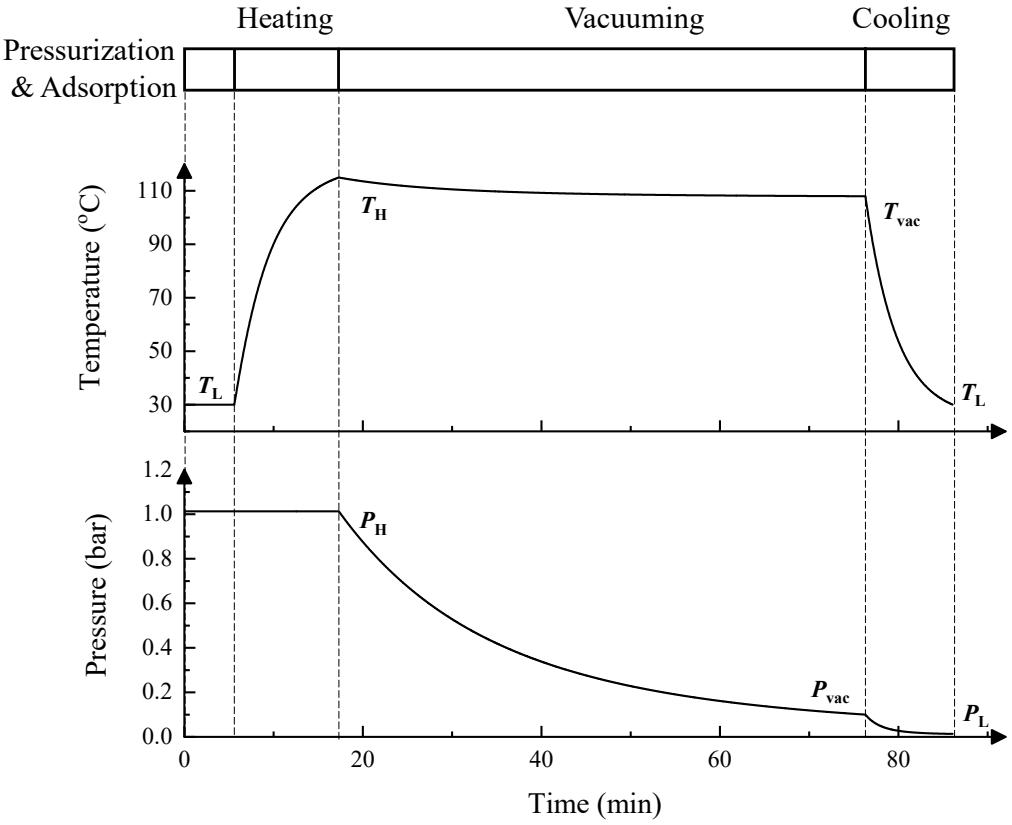

Figure S2. *Temperature and pressure variations with time in the TVSA process.*

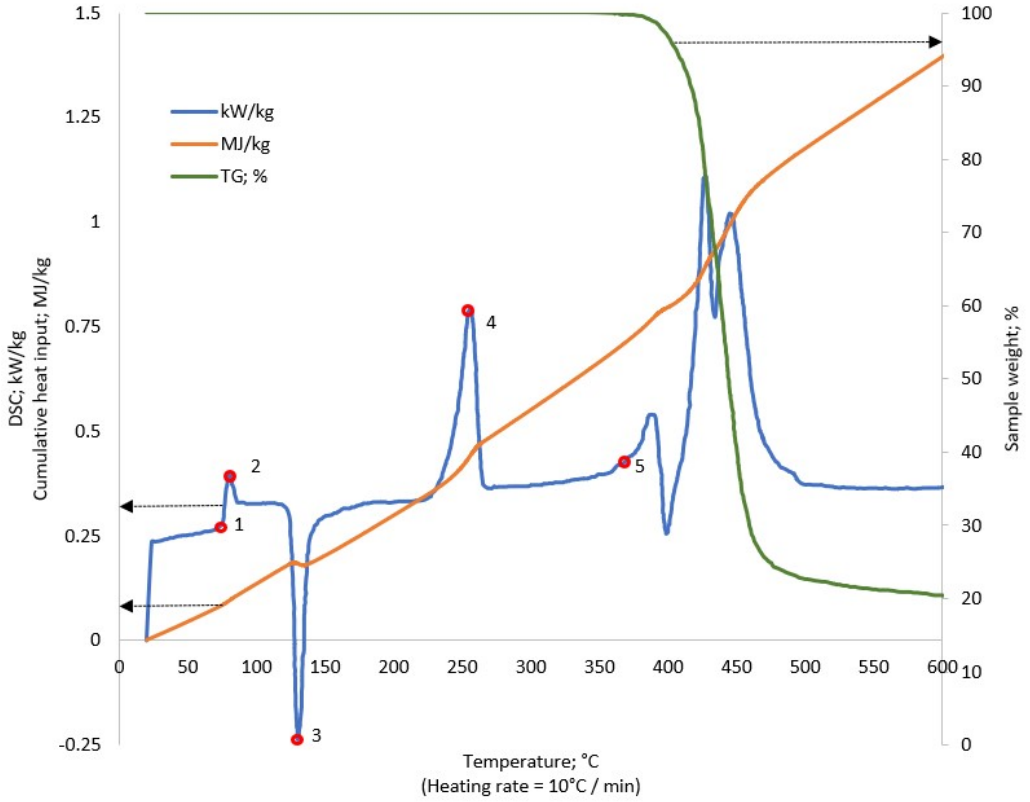

Figure S3. *Differential scanning calorimetry (DSC) trace of a pure PET sample (blue line), reproduced from the instrument application sheet [S41]. Temperature points 1–5 indicate glass transition (76 °C), relaxation (81 °C), cold crystallization (131 °C), melting (255 °C), and pyrolysis initiation (360 °C), respectively. The energy required for a sample to achieve a certain temperature at a constant heating rate of 10 °C/min is shown with cumulative heat input in MJ/kg (orange line). The loss of mass due to thermal decomposition is shown as a percentage by the green thermogravimetry (TG) line. To reach 600 °C, 1 kg of PET requires ~1.4 MJ of thermal energy with an additional ~1.17 MJ to maintain decomposition at 600 °C within 1 h.*

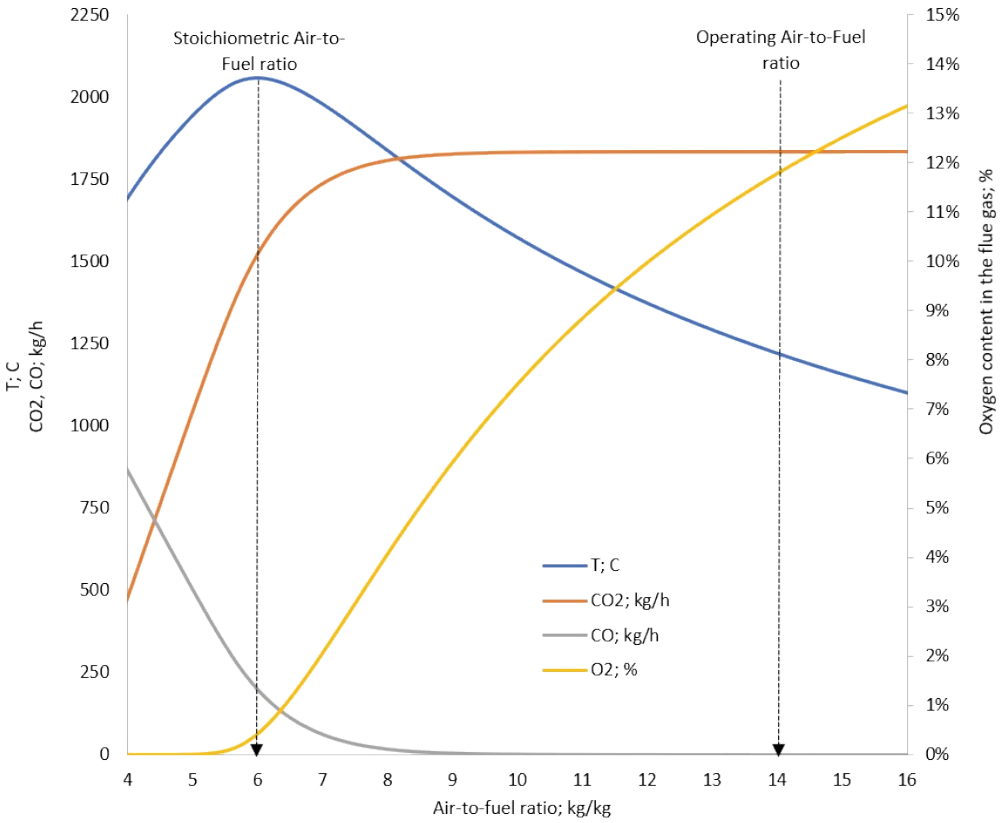

Figure S4. *Results of a parametric sensitivity analysis simulation of pyrolysis vapors and a mixture of non-condensable gases with varying air-to-fuel (ATF) ratio. The operating ATF ratio was set to ~14 wt./wt. to insure complete combustion of all volatile organic compounds. The NO level at operating ATF ratio was 0.0876 wt.% of the flue gas. The lower heating value of 19.22 MJ/kg was determined to be the heat released from combusting the fuel mixture (pyrolysis vapors + non-condensable gases) with a stoichiometric quantity of air and by cooling the flue gases to 150 °C. Using the same principle, the lower heating values for pyrolysis vapors and non-condensable gasses were individually determined to be 25.07 MJ/kg and 9.05 MJ/kg, respectively.*

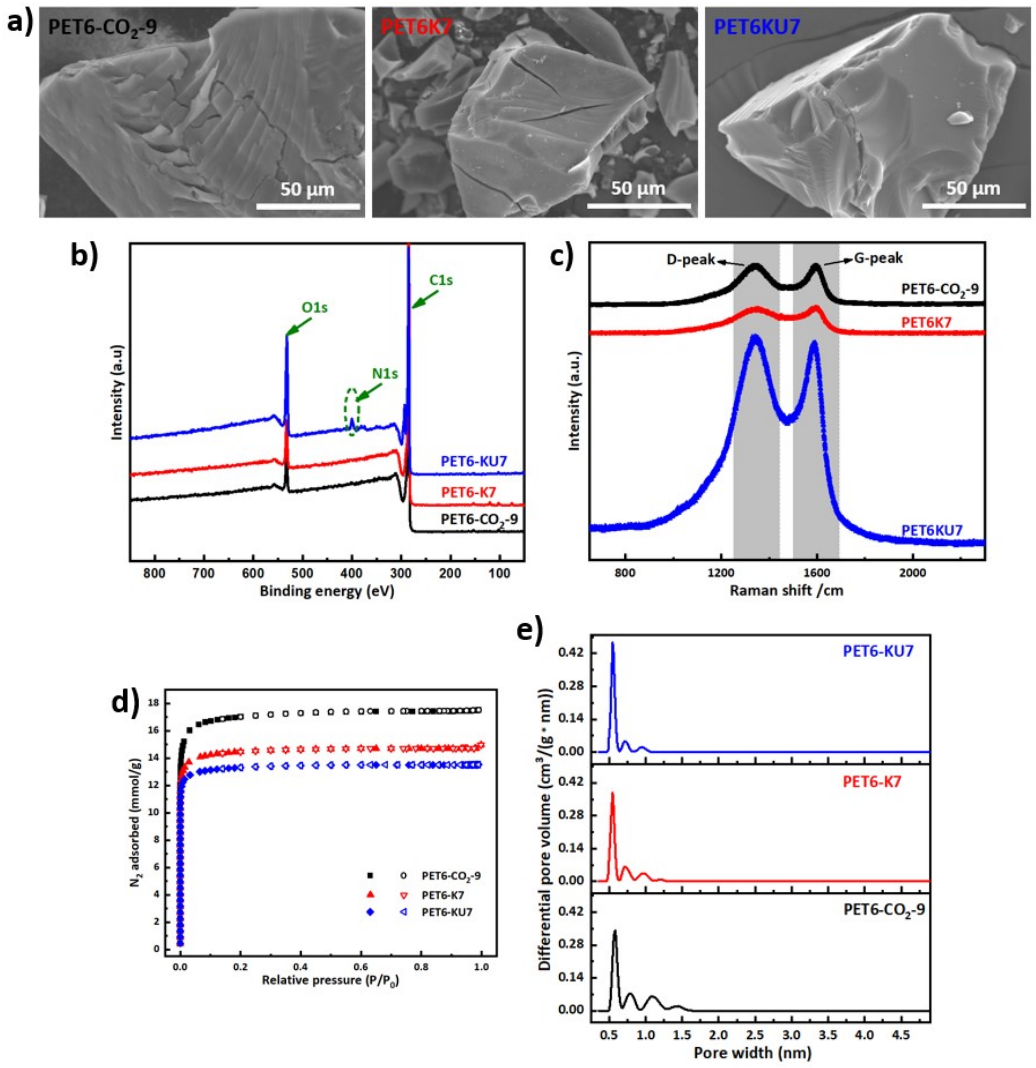

Figure S5. *a) Scanning electron microscope images, b) X-ray photoelectron spectroscopy full survey. c) Raman spectra. d) N_2 adsorption isotherms (solid symbols) and desorption isotherms (open symbols) at -196 °C e) Pore size distributions (PSDs) in waste PET plastic-derived porous carbons (WPDPCs). Note that all data for PET6-K7 and PET6-KU7 were derived from a previous publication [S1].*

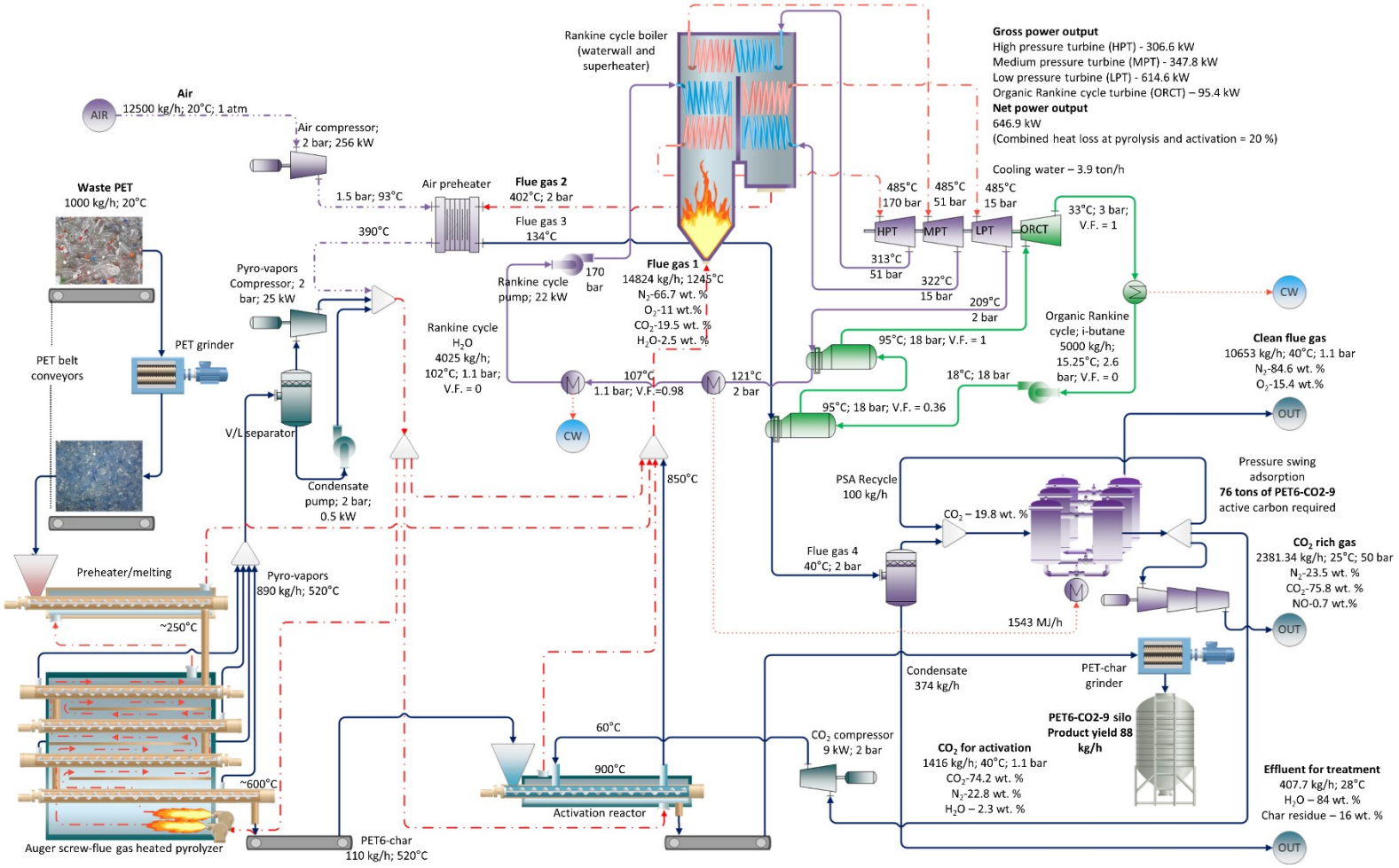

Figure S6. *Process flow diagram of the PET6-CO_2-9 porous carbon production process and flue gas CO_2 capture of a representative 1 t/h PET waste scale. Blue streamlines and unit operations indicate pyrolysis and activation processes. Purple streamlines and operations indicate the primary power (Rankine) cycle and CO_2 capture. Green streamlines indicate the secondary power (organic Rankine) cycle and a heat sink for the flue gas before the CO_2 capture process. Red streamlines indicate the primary heat sources for the process (lines and dots) and major heat duties of the unit operations (dots only).*

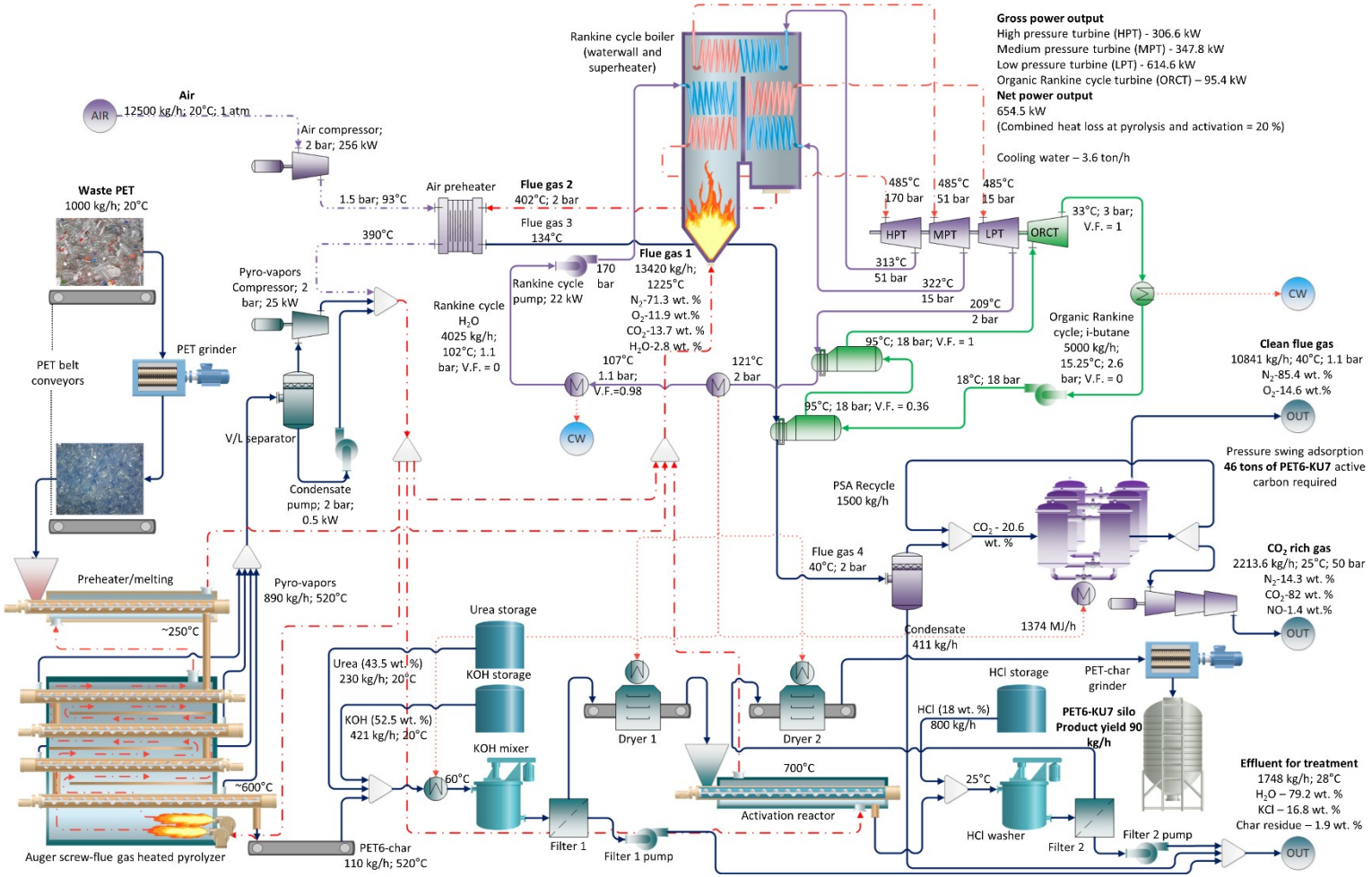

Figure S7*. Process flow diagram of the PET6-KU7 porous carbon production process and flue gas CO_2 capture of a representative 1 t/h PET waste scale. Blue streamlines and unit operations indicate pyrolysis and activation processes. Purple streamlines and operations indicate the primary power (Rankine) cycle and CO_2 capture. Green streamlines indicate the secondary power (organic Rankine) cycle and a heat sink for the flue gas before the CO_2 capture process. Red streamlines indicate the primary heat sources for the process (lines and dots) and major heat duties of the unit operations (dots only).*

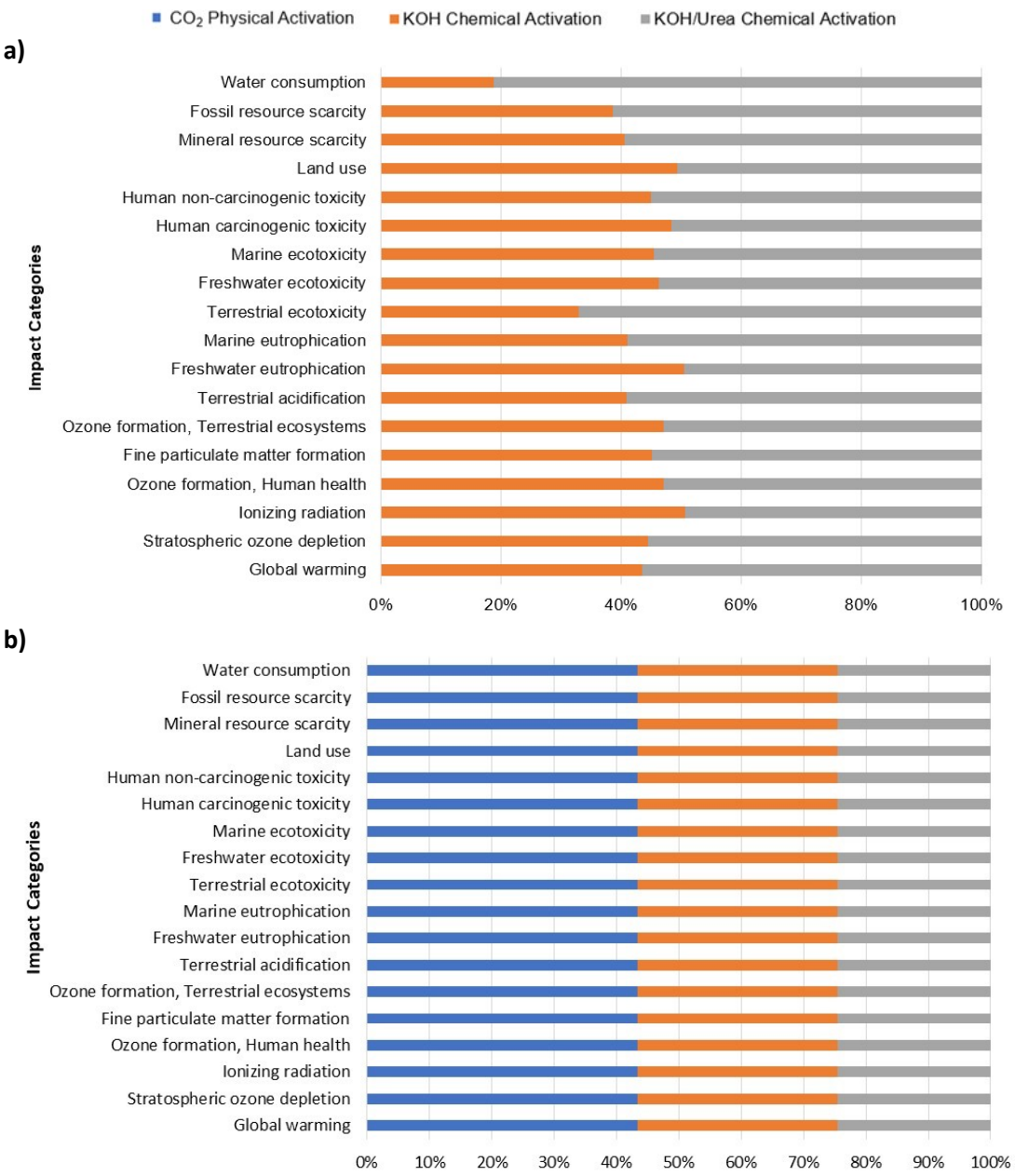

***Figure S8**. Midpoint assessment results of the physical and two chemical activation methods used to produce activated porous carbon material and capture "kg of CO_2 captured by WPDPCs" using the ReCiPe (H) impact assessment method: a) environmental impacts for the three methods; b) mitigated environmental for the three activation methods and is due to the reduction in energy from the national energy mix. The LCA results for the three activation methods shown here do not account for any additional approaches for the disposal of CO_2 emissions from the production unit; however, some emitted CO_2 was reused within the physical activation process and the leftover emissions were disposed of using a carbon capture facility. In this process, we observed that the adsorption properties of each porous carbon were different. For this reason, our functional unit (FU) is "kg of CO_2 captured by WPDPC." In addition, to evaluate the mitigated environmental impacts related to energy consumption, we used the same FU. Note: The results are stacked for the three activation unit processes. Each colored bar represents the percentage contribution of an activation method unit process to a given impact category. The stacked contribution for the life cycle of CO_2 physical activation is zero because of the reuse of the produced CO_2 by the production unit.*

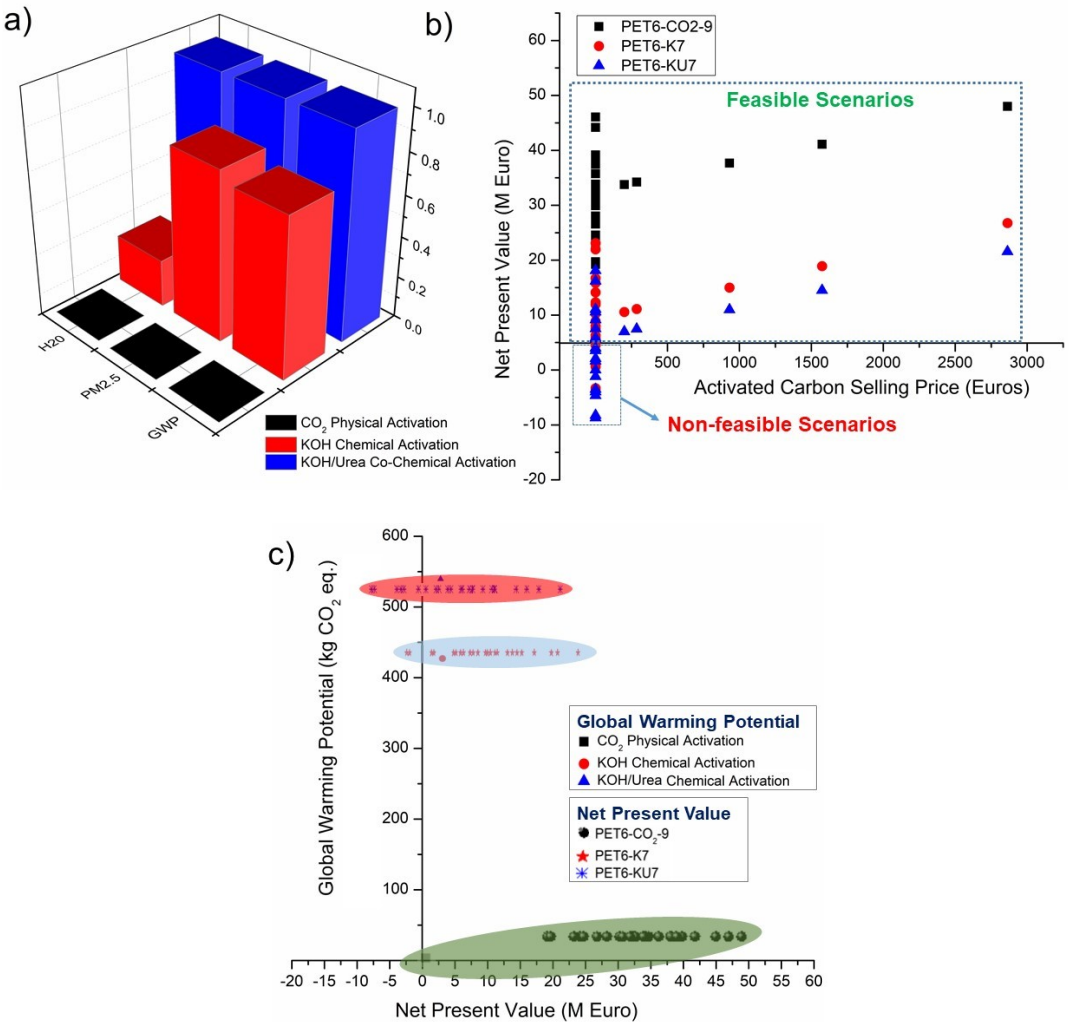

Figure S9. *a) Normalized values of the selected impact categories (global warming potential [GWP], fine particulate matter formation [PM2.5], and water consumption [H_2O]) of the three activation pathways. b) Clusters of net present values (NPVs) of the waste PET-derived activated material denoting variations in activated carbon selling prices and heat losses in the system that would affect power generation. The thick dotted blue box indicates all of the feasible scenarios, and the thin dotted line blue box represents the non-feasible scenarios. c) Clusters of feasible scenarios as revealed by the integrated life-cycle assessments and techno-economic assessments. The red ellipse represents higher environmental impacts and lower economic benefits, the light blue ellipse represents the moderate environmental impacts with considerable economic benefits, and the green ellipse represents lower environmental impacts with higher economic benefits.*

References

S1. X. Yuan, S. Li, S. Jeon, et al., *J. Hazard. Mat.*, 2020, **399**, 123010.
S2. D. Tiwari, C. Goel, H. Bhunia, P. K. Bajpai, *J. Environ. Manage.,* 2017, **197**, 415-427.
S3. A. L. Chaffee, G. P. Knowles, Z. Liang, et al., *Int. J. Greenh. Gas Con.*, 2007, **1**, 11-18.
S4. R. Zhao, L. Liu, L. Zhao, S. Deng, et al., *Renew. Sust. Energ. Rev.*, 2019, **114**, 109285.
S5. R. Zhao, S. Deng, Y. Liu, et al., *Energy*, 2017, **119**, 1131-1143.
S6. L. Jiang, R. Q. Wang, A. Gonzalez-Diaz, et al., *Appl. Therm. Eng.*, 2020, **169**, 114973.
S7. R. Bai, M. Yang, G. Hu, L. Xu, Z. Li, S. Wang, W. Dai, M. Fan, *Carbon*, 2015, **81**, 465-473.
S8. G. Singh, J. Lee, A. Karakoti, R. Bahadur, et al., *Chem. Soc. Rev.,* 2020, **49**, 4360-4404.
S9. L. Rao, S. Liu, L. Wang, C. Ma, J. Wu, L. An, X. Hu, *Chem. Eng. J.*, 2019, **359**, 428-435.
S10. H. Wei, J. Chen, N. Fu, H. Chen, H. Lin, S. Han, *Electrochim. Acta*, 2018, **266**, 161-169.
S11. B. Kaur, R. K. Gupta, H. Bhunia, *Micropor. Mesopor. Mat.,* 2019, **282**, 146-158.
S12. B. Kaur, J. Singh, R. K. Gupta, H. Bhunia, *J. Environ. Manage.,* 2019, **242**, 68-80.
S13. X. Yuan, J. G. Lee, H. Yun, S. Deng, et al., *Chem. Eng. J.*, 2020, **397**, 125350.
S14. A. Rehman, S.-J. Park, *Chem. Eng. J.,* 2019, **362**, 731-742.
S15. S. Li, S. Deng, R. Zhao, L. Zhao, et al, *Energy*, 2019, **179**, 876-889.
S16. A. Ajenifuja, L. Joss, M. Jobson, *Ind. Eng. Chem. Res.*, 2020, **59**, 3485-3497.
S17. E. Ansah, L. Wang, A. Shahbazi, *Waste Manage.,* 2016, **56**, 196-206.
S18. S. Du, J. A. Valla, R. S. Parnas, G. M. Bollas, *ACS Sustain. Chem. Eng.,* 2016, **4**, 2852-2860.
S19. J. Lee, T. Lee, Y. F. Tsang, J.-I. Oh, E. E. Kwon, *Energ. Convers. Manage.,* 2017, **148**, 456-460.
S20. J. Chattopadhyay, T. S. Pathak, R. Srivastava, A. C. Singh, *Energy,* 2016, **103**, 513-521.
S21. M. Pohorely, M. Vosecky, P. Hejdova, et al., *Fuel,* 2006, **85**, 2458-2468.
S22. D. Oh, H. W. Lee, Y.-M. Kim, Y.-K. Park, *Energy Procedia,* 2018, **144**, 111-117.
S23. L. Chen, S. Wang, H. Meng, Z. Wu, J. Zhao, *Energy Procedia,* 2017, **105**, 391-397.
S24. R. K. Singh, B. Ruj, A. K. Sadhukhan, P. Gupta, *J. Energy Inst.,* 2020, **93**, 1020-1035.
S25. M. Azam, S. S. Jahromy, W. Raza, et al., *Environ. Int.,* 2020, **134**, 105291.
S26. A. Dhahak, G. Hild, M. Rouaud, G. Mauviel, V. Burkle-Vitzthum, *J. Anal. Appl. Pyrol.,* 2019, **142**, 104664.
S27. M. Dzięcioł, J. Trzeszczyński, *J. Appl. Polym. Sci.,* 2001, **81**, 3064-3068.
S28. A. Dhahak, V. Carre, F. Aubriet, G. Mauviel, V. Burkle-Vitzthum, *Ind. Eng. Chem. Res.,* 2020, **59**, 1495-1504.
S29. Y. Yang, J. Wang, K. Chong, A. V. Bridgwater, *Energ. Convers. Manage.,* 2018, **174**, 406-416.
S30. P. C. Badger, ORNL/TM-2002/199, 2002, DOE/EERE 10.2172/814666.

S31. M. M. Wright, D. E. Daugaard, J. A. Satrio, P. C. Brown, *Fuel,* 2010, **89**, S2-S10.
S32. Y. Yang, J. G. Brammer, D. G. Wrigh, et al., *Appl. Energ.,* 2017, **191**, 639-652.
S33. R. Rowshanzadeh, Master thesis from KTH Sweden, 2010, 1-101.
S34. B. F. Tchanche, S. Quoilin, S. Declaye, G. Papadakis, V. Lemort, *In Eng. System. Des. Anal.,* 2010, **49156**, 249-256.
S35. T. Haeldermans, L. Campion, T. Kuppens, et al., *Bioresource Technol.,* 2020, **318**, 124083.
S36. Price Monitoring Center, NDRC. China CN: Usage Price: Industrial Use Water: Tianjin from Jan. 2003 to Nov. 2019. https://www.ceicdata.com/en/china/price-monitoring-center-ndrc-transaction-price-production-material-water-industrial-use/cn-usage-price-industrial-use-water-tianjin.
S37. D. C. Ko, E. L. Mui, K. S. Lau, G. McKay, *Waste Manage.,* 2004, **24**, 875-888.
S38. T. Thewys, T. Kuppens, *Int. J. Phytoremediat.,* 2008, **10**, 561-583.
S39. M. S. Peters, K. D. Timmerhaus, R. E. West, McGraw-Hill New York, 1968, Vol. 4.
S40. X.-g. Zhao, G.-w. Jiang, A. Li, L. Wang, *Waste Manage.,* 2016, **48**, 604-618.
S41. NETZSCH-Gerätebau GmbH, 2008, www.netzsch.com.